



Preparation and biocompatibility of electrospun poly(L-lactide-co- ϵ -caprolactone)/fibrinogen blended nanofibrous scaffolds

Zhengdong Fang, Weiguo Fu*, Zhihui Dong, Xiangman Zhang, Bin Gao, Daqiao Guo, Hongbing He, Yuqi Wang

Department of Vascular Surgery, Zhongshan Hospital, Fudan University, 180 Fenglin Road, Shanghai 200032, China

ARTICLE INFO

Article history:

Received 25 August 2010
Received in revised form 1 December 2010
Accepted 1 December 2010
Available online 9 December 2010

Keywords:

Electrospinning
Tissue engineering
Nanofibrous scaffold
Natural polymer
Synthetic polymer

ABSTRACT

Electrospun blended nanofibrous scaffolds were fabricated from an synthetic biodegradable polymer (poly(L-lactide-co- ϵ -caprolactone): PLCL; 8% solution) and a natural protein (fibrinogen; 100 mg/ml solution) with different volume ratios. Results showed that the blended scaffolds consisted of nanoscale fibers with mean diameters ranging from 224 to 450 nm. The deposition of the fibrinogen amino groups on the surfaces of the blended scaffolds was confirmed by XPS. The hydrophilicity of the blended scaffolds were improved with the fibrinogen content increasing in the blended system. Cell viability assay and SEM results showed that human umbilical vein endothelial cells (HUVECs) had progressive growth and well spread morphology on the blended scaffolds. This study demonstrated that electrospun PLCL/fibrinogen blended scaffolds have potential application in tissue engineering.

© 2010 Elsevier B.V. All rights reserved.

1. Introduction

The principle of designing of scaffolds for tissue engineering is to mimic the structure and biological function of the native extracellular matrix (ECM) with appropriate mechanical and biological properties. With the goal of mimicking the ECM geometry, nanofibrous scaffolds have already been designed to serve as a suitable environment for cell attachment and proliferation [1]. Presently, several methods, including phase separation, self-assembly and electrospinning, are used to fabricate polymeric nanofibers [2–4]. Among these, electrospinning is considered more economical and simple, and appears to be a very reasonable technique for fabricating nanofibrous scaffolds from a variety of polymer solutions. The resulting artificial scaffolds not only mimic the features of the ECM, but also provide high surface-to-volume ratios and the potential for high porosity and interconnected pores to support cell growth and infiltration [5,6].

Over the past few years, a wide range of synthetic polymers (polyglycolic acid (PGA), polylactide (PLA), polycaprolactone (PCL)) [7,8] and natural polymers (collagen, chitosan, fibrinogen) [9,10] as well as their composites have been used to fabricate nanofibrous scaffolds for tissue engineering. Poly(L-lactide-co- ϵ -caprolactone) (PLCL), a random copolyester of lactide and ϵ -caprolactone, is a highly elastomeric synthetic biodegradable polymer that has been

of great interest for soft flexible tissue engineering, such as cardiovascular, cartilage and nerve regeneration [11,12]. However, adhesive proteins and specific ligands for cell-ECM interactions, which are critical for cell migration, cell proliferation and subsequent tissue remodeling, are absent from the surface of PLCL. In order to enhance its biocompatibility, PLCL needs to be modified with adhesive proteins and structural proteins to incorporate their biological activities. There are many methods for enhancing cell adhesion and proliferation on synthetic polymers by modifying the synthetic polymer surface, including physical coating and chemical treatments [13–15]. However, these surface modification techniques have the drawbacks of slow mass transference of proteins into the three-dimensional porous materials and low stability. Compared with these surface modification techniques, direct electrospinning of blended synthetic and natural polymers has the potential to readily refine the composition of the nanofibers by adding bioactive proteins such as collagen, gelatin and growth factors. Moreover, the existence of bioactive proteins on the surface of and inside the nanofibers confers remarkable ability as a matrix for cell migration and provides sustained cell recognition signals with polymer degradation, which is important for cell function [16]. Fibrinogen is a naturally occurring plasma protein with a molecular mass of 340 kDa, and its major function is the formation of fibrin fibers that play vital roles in subsequent wound healing responses and ECM remodeling [17]. Previously, fibrinogen-based scaffolds have been developed in the form of fibrin gels, which require mixing of cells into the fibrinogen solution prior to the formation of a hydrogel. Recently, fibrinogen has been successfully electrospun

* Corresponding author. Tel.: +86-21-64041990x2168; fax: +86-21-64038038.
E-mail address: fu.weiguo@hotmail.com (W. Fu).

Table 1
Concentrations of PLCL and fibrinogen in the mixed solutions.

PLCL/fibrinogen ratio (V/V)	Mass in 100 ml HFIP		Fibrinogen mass ratio (w/w) (%)	Total solute concentration (w/v) (%)
	PLCL (g)	Fibrinogen (g)		
Pure PLCL	8	0	0	8
4:1	6.4	2	23.81	8.4
2:1	5.33	3.33	38.45	8.66
1:1	4	5	55.56	9
1:2	2.67	6.67	71.41	9.34
Pure fibrinogen	0	10	100	10

for the fabrication of nanofibrous scaffolds that mimic the structure of the native ECM. The resulting nanofibrous scaffolds have been shown to support cell proliferation and to promote cell interactions, but have weak mechanical properties [18,19]. To date, however, there is limited information regarding the use of PLCL/fibrinogen nanofibrous scaffolds for tissue engineering.

In the present study, we aimed to fabricate novel electrospun blended nanofibrous scaffolds composed of PLCL and fibrinogen to obtain better biodegradable materials by combining their respective advantages. More specifically, we aimed to enhance the biocompatibility of PLCL with the bioactivity of fibrinogen. We evaluated the microscopic morphologies, cell attachment and proliferation of the obtained electrospun PLCL/fibrinogen blended scaffolds, and finally these blended scaffolds were shown to have potential application in tissue engineering.

2. Experimental

2.1. Materials

The random copolymer of PLCL (70:30), which has composition of 70 mol% L-lactide, was purchased from Daigang Bio-Tech Co. Ltd. (Jinan, China). The number average molecular weight (M_n) and weight average molecular weight (M_w) were determined by gel-permeation chromatography (Model 410; Waters, USA) to be 222×10^3 and 387×10^3 , respectively. Lyophilized bovine fibrinogen were obtained from Sigma-Aldrich Chemical Co. Ltd. (USA). The solvent 1,1,1,2,2,2-hexafluoro-2-propanol (HFIP; purity, $\geq 99.0\%$) was obtained from Yumei Co. Ltd. (Shanghai, China). A Cell Counting Kit-8 (2-(2-methoxy-4-nitrophenyl)-3-(4-nitrophenyl)-5-(2,4-disulfophenyl)-2H-tetrazolium; WST-8) was obtained from Dojindo Laboratories (Japan). Cell medium ingredient and live/dead cell viability assay kit was obtained from Invitrogen Corp. (USA).

2.2. Preparation of the electrospinning solutions

A PLCL solution (8% w/v) was obtained by dissolving PLCL in HFIP. A fibrinogen solution was prepared as described previously [20]. Fibrinogen was dissolved in 9 parts HFIP and 1 part 10 minimal essential medium (Gibco Invitrogen, USA) at a concentration of 100 mg/ml. A series of PLCL/fibrinogen electrospinning solutions was then obtained by mixing the two solutions at volume ratios of PLCL to fibrinogen at 4:1, 2:1, 1:1, and 1:2 respectively. The calculated concentrations for each of the components in the various samples are listed in Table 1. For convenience, all the descriptions are expressed as volume ratios in the following sections.

2.3. Electrospinning

The electrospinning process was performed using a Nanofiber Electrospinning Unit (Kato-Tech Corp., Japan). The setup consisted of a high-voltage power supply, an infusion pump, a syringe and a rotating mandrel. The solution for each group was loaded into a 10-ml syringe with a 22-gauge stainless-steel blunt-ended nee-

dle. The needle was connected to the high-voltage power supply, which was able to generate positive difference voltages (0–30 kV) between the syringe and the rotating mandrel. For electrospinning of PLCL/fibrinogen composite fibers, the flow rate was 2–3 ml/h. The distance between the needle tip and the rotating mandrel (diameter: 6 cm; length: 20 cm; 303 polished stainless-steel; rotation: 500 rpm) was in the range of 12–15 cm and the positive voltage applied to the polymer solutions was in the range of 25–30 kV. The electrospun fibers were collected on the rotating mandrel covered with aluminum foil. To evenly coat the mandrel, the syringe pump was traversed at a speed of 10 mm/min. All experiments were performed at room temperature. Subsequently, all the electrospun fibers were vacuum-dried for 48 h at room temperature and stored in desiccators.

2.4. Characterization

The morphology and diameter of the electrospun scaffolds were evaluated using a Stereoscan 360 scanning electron microscope (SEM) (Cambridge, UK). Platinum was sputter-coated onto the surface of the samples before the SEM observation. The SEM scanning was performed at an accelerating voltage of 10 kV. The average diameters of the fibers were obtained by measuring 40 randomly selected fibers on the electron micrographs using Image J, an open source image analysis software available from the National Institutes of Health (NIH).

The surface compositions of the composite fibrous membranes were analyzed by X-ray photoelectron spectroscopy (XPS) using a PHI-5000C ESCA system (PerkinElmer, USA). Binding energies were calibrated by using the containment carbon ($C1s = 284.6$ eV). Three samples were used for each group.

For determination of hydrophilicity of scaffolds, the contact angles of the electrospun scaffolds were measured by a contact angle analyzer (Dataphysics, Germany). The droplet of 5 μ l deionized water was deposited on the surface of the samples. Three droplets on each sample and five samples for each group were measured.

2.5. Cell isolation and culture

Human umbilical vein endothelial cells (HUVECs) were isolated from freshly harvested umbilical cords as described previously [21]. The project was approved by the Ethics Committee of Zhong Shan Hospital, Fudan University. Briefly, HUVECs were obtained by digestion with collagenase type I (1 mg/ml; Sigma, USA) for 10 min at 37 °C. After the isolation, the cells were seeded in complete medium consisting of M199 supplemented with 10% heat-inactivated fetal bovine serum, 25 ng/ml basic fibroblast growth factor (R&D Systems, USA) and 1% penicillin-streptomycin, and incubated in a humidified atmosphere of 5% CO_2 at 37 °C. HUVECs were identified by positive staining with a mouse anti-human von Willebrand factor monoclonal antibody (Santa Cruz Biotechnology, USA). The cells were passaged when they reached 80% confluence, and cells at passages 3–5 were used in experiments.

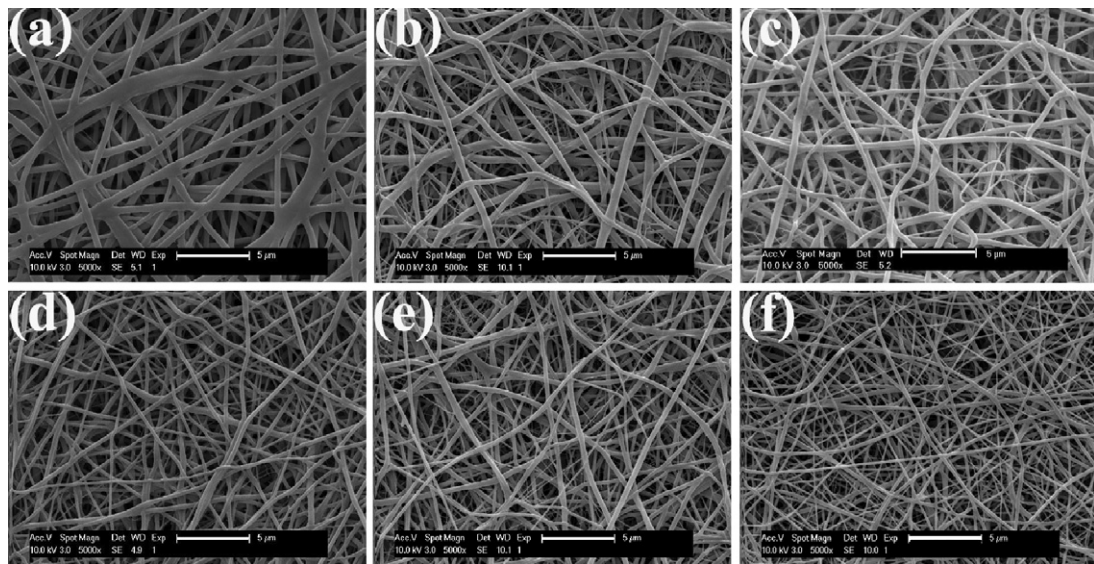


Fig. 1. SEM micrographs of electrospun PLCL/fibrinogen blended fibrous scaffolds. (a) Pure PLCL. (b) PLCL/fibrinogen, 4:1. (c) PLCL/fibrinogen, 2:1. (d) PLCL/fibrinogen, 1:1. (e) PLCL/fibrinogen, 1:2. (f) Pure fibrinogen. Scale bars, 5 μm .

2.6. Cell adhesion and proliferation assays

Electrospun nanofibrous scaffolds were punched into round sections with a diameter of 6 mm, and sterilized by soaking in 75% ethanol for 15 min. After rinsing thoroughly with sterile phosphate-buffered saline (PBS) five times, the electrospun scaffold sections were placed in 96-well culture plates, soaked in serum-free medium for 1 h at room temperature and rinsed with PBS. To evaluate adhesion and proliferation, HUVECs were seeded into the 96-well plates at 6×10^3 cells/well and incubated at 37 °C in a 5% CO₂ atmosphere. The medium was changed every 2–3 days during the culture period. The number of viable cells was measured using a commercially available Cell Counting Kit-8 (WST-8). The principal mechanism of this assay is that metabolically active cells react with a tetrazolium salt in the WST-8 reagent to produce a soluble formazan dye that gives an absorbance at a wavelength of 450 nm. For cell adhesion tests, the samples were incubated for 4 h. For cell proliferation tests, the scaffolds were cultured for 1, 3, 5 and 7 days. At each time point, the medium was replaced with fresh medium containing 10% WST-8 according to the manufacturer's instructions. After 3 h of incubation, the absorbances were measured at 450 nm using a microplate reader (Model 550; Bio-Rad, USA) with a reference wavelength of 655 nm and compared with a standard curve to calculate the cell numbers. Tissue culture polystyrene (TCPS) without any scaffolds was used as a control. For each experiment, four samples were evaluated.

2.7. Cell viability assay

After 7 days in culture, the viabilities of HUVECs on nanofibrous scaffolds were examined by live/dead cell viability assays. Briefly, scaffolds seeded with cells were washed with PBS, and then incubated in 1 μM calcein AM (to stain live cells) and 4 μM ethidium-1 (to stain dead cells) in PBS at room temperature for 30 min. The stained cells were observed using a DMIRE2 confocal microscope with a TCS SP2 scanner (Leica Microsystems, Germany).

2.8. Cell behavior on nanofibrous scaffolds

Cellular fibers were harvested after 7 days in culture to study the morphological characteristics of the cells on the electrospun fibers. The scaffolds were washed three times with PBS to remove nonad-

herent cells and then fixed in 4% paraformaldehyde overnight. After washing with PBS, the samples were dehydrated through a graded series of ethanol solutions, followed by critical-point drying. The samples were then sputtered with gold and visualized using an SEM (Model S520; Hitachi, Japan) at an accelerating voltage of 20 kV.

2.9. Statistical analysis

All data were expressed as means \pm standard deviation (SD). Statistical analyses were carried out by one-way ANOVA with a Games–Howell post hoc test. Differences were considered to be statistically significant for values of $p < 0.05$.

3. Results and discussion

3.1. Morphology of the nanofibrous scaffolds

Electrospinning has gained popularity in the tissue engineering community because it has the ability to produce nanoscale and submicron fibers that mimic the structure of the natural ECM. The morphology of electrospun fibers is typically influenced by the properties of the polymer solutions, including the concentration, surface tension and viscosity [22–24]. Fig. 1 shows the morphologies of electrospun PLCL, fibrinogen and composite PLCL/fibrinogen scaffolds. The average diameters of these electrospun fibers are shown in Table 2. For all the volume ratios tested in this study, PLCL and fibrinogen were successfully electrospun to form non-woven and interconnected networks, with relatively uniform and randomly oriented fibers. Analyses showed that the average diameter of fibers of the scaffolds decreased with increasing content

Table 2
Fiber diameters and water contact angles of the PLCL/fibrinogen blended scaffolds.

PLCL/fibrinogen ratio (v/v)	Fiber diameter (nm)	Water contact angle (°)
Pure PLCL	450 \pm 135	105.07 \pm 6.03
4:1	329 \pm 125*	87.73 \pm 5.82*
2:1	306 \pm 91*	72.93 \pm 3.33*
1:1	283 \pm 71*	58.93 \pm 4.71*
1:2	279 \pm 81*	41.47 \pm 3.85*
Pure fibrinogen	225 \pm 56	0

Notes: Data are expressed as mean \pm SD. * $p < 0.01$, for comparisons between the blended and pure PLCL scaffolds.

Table 3
Atom ratios of electrospun fibrous scaffolds determined by XPS.

PLCL/fibrinogen ratio(V/V)	Carbon atomic ratio (%)	Nitrogen atomic ratio (%)	Oxygen atomic ratio (%)	Sulfur atomic ratio (%)
Pure PLCL	67.35	0	32.65	0
4:1	67.71	2.13	30.08	0.05
2:1	68.21	3.19	28.4	0.14
1:1	67.17	4.71	28.11	0.21
1:2	66.26	8.43	25.01	0.28
Pure fibrinogen	65.47	14.73	18.51	0.65

of fibrinogen in the blended scaffolds ($p < 0.05$). In detail, the average diameters were estimated to be 450 ± 135 , 329 ± 125 , 306 ± 91 , 283 ± 71 , 279 ± 81 , and 224 ± 56 nm for PLCL/fibrinogen volume ratios of 1:0, 4:1, 2:1, 1:1, 1:2, and 0:1, respectively. These results demonstrated that the concentration of fibrinogen had a direct relation with the fiber morphology. This phenomenon could be explained by the conductivity increase of the blended solution. Fibrinogen is a typical amphiprotic macromolecule electrolyte. When fibrinogen was added, higher charge densities of the blended solutions could be carried under an electrical field. It has been found that increases in conductivity and charge density can lead to the imposition of stronger elongation forces on the solutions because of the self-repulsion of the excess charges under the electrical field, thereby resulting in substantially smaller diameters of the electrospun fibers [25].

3.2. XPS analyses

To investigate the surface properties of the composite scaffolds, the existence of fibrinogen on the scaffold surfaces was verified through XPS via the presence of amino groups. Elemental scans were carried out for carbon, nitrogen, oxygen, and sulfur. Table 3 shows the atomic ratios of the blended scaffolds, together with those of pure PLCL and pure fibrinogen scaffolds. The results verified that nitrogen and sulfur atoms were absent from the surface of the pure PLCL scaffolds. This was consistent with the chemical structure of PLCL. The PLCL/fibrinogen blended scaffolds contained carbon, oxygen, nitrogen, and sulfur elements. Furthermore, the nitrogen and sulfur amounts increased from 2.13% and 0.05% for PLCL/fibrinogen (4:1) to 8.43% and 0.28% for PLCL/fibrinogen (1:2), respectively. Pure fibrinogen scaffolds contained the highest amounts of nitrogen (14.73%) and sulfur (0.65%). The existence of fibrinogen on the surface of and inside the nanofibers confers on it a remarkable matrix property that allows for cell migration and provides sustained cell recognition signals with polymer degradation, which is important for cell function [26].

3.3. Water contact-angle measurements

To understand the hydrophilicity changes of the electrospun PLCL/fibrinogen scaffolds with respect to amounts of PLCL and fibrinogen, static water-contact angles were measured (Table 2). A smaller contact angle usually means that the scaffold surface is more hydrophilic. As expected, the electrospun PLCL scaffolds had a highest contact angle measurement ($105.07 \pm 6.03^\circ$), and the water droplets were rapidly absorbed into the fibrinogen scaffolds because of their hydrophilic groups. The incorporation of fibrinogen significantly decreased the contact angle of the blended scaffolds ($p < 0.05$). When the blended ratio of PLCL/fibrinogen changed from 4:1 to 1:2, the contact angle decreased from $87.73 \pm 5.82^\circ$ to $41.47 \pm 3.85^\circ$. Our results demonstrated that the incorporation of fibrinogen significantly improved the hydrophilicity of the scaffolds. This might be attributed to the amine and carboxylic functional groups in fibrinogen structure whereas such functional groups are not present in PLCL structure. Many works have indicated that the surface hydrophilicity plays an essential role in cell

growth on biomaterials [27,28]. Such a property will be extremely useful for cell seeding.

3.4. In vitro cell culture experiments

Cell-scaffold interactions were studied in cell culture by seeding HUVECs on the various electrospun scaffolds for one week. Fig. 2 shows the data for the cell adhesion and proliferation of HUVECs after seeding on different electrospun scaffolds and TCPS controls during seven days in culture. The cell numbers at 4 h indicate the initial cell adhesion. It was found that HUVECs exhibited higher cell adhesion to the PLCL scaffolds compared with the blended scaffolds during the first 4 h ($p < 0.05$). The incorporation of fibrinogen improved the hydrophilicity of the scaffolds. Generally, hydrophobic surfaces are able to absorb more proteins in the first step to provide a better cell adhesion environment [29]. However, the cell proliferation showed different behavior. After culturing for 1 day, the HUVECs on all scaffolds adhered to some extent and began to proliferate, but there were no significant differences between the cell number on the PLCL scaffolds and that on the PLCL/fibrinogen blended scaffolds ($p > 0.05$). After culturing for 3 and 5 days, the cell number on the PLCL/fibrinogen blended scaffolds increased quickly. The cell proliferation on the blended scaffolds exhibited the significant higher proliferation rate than that on the PLCL scaffolds ($p < 0.01$), and the HUVECs on the PLCL/fibrinogen (2:1) scaffolds showed the highest proliferation rate. After culturing for 7 days, the HUVECs continue to proliferate. By comparing the cell numbers after seven days of culture with the initial number of seeded cells (6×10^3 cells/well), the proliferation rates for the PLCL/fibrinogen (4:1), (2:1), (1:1), and (1:2) scaffolds were found to be 3.23-, 4.35-, 3.95-, and 3.39-fold, respectively, which were significantly higher than that on the PLCL scaffolds (1.98-fold) ($p < 0.01$), and the cell proliferation rate on the PLCL/fibrinogen (2:1) scaffolds were the highest. It has been known that fibrinogen are attractive scaffold materials for tissue engineering applications because they are biocompatible and biodegradable and have high affinities for var-

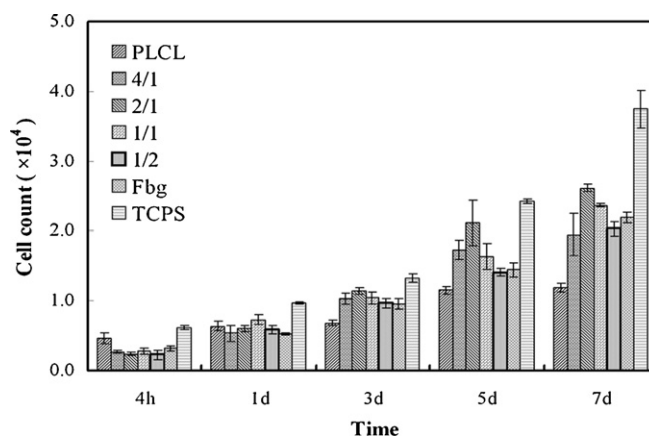


Fig. 2. Metabolic activities of HUVECs cultured on electrospun PLCL/fibrinogen blended fibrous scaffolds evaluated by WST-8 assays. Data are expressed as means \pm SD ($n = 3$).

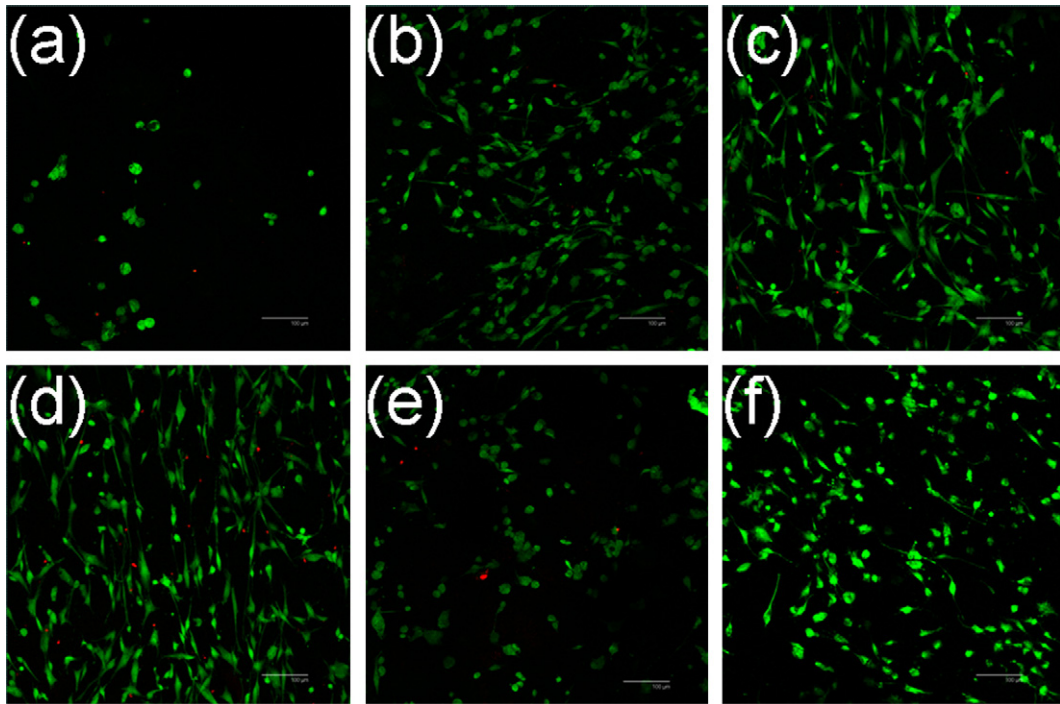


Fig. 3. Viabilities of HUVECs cultured on electrospun PLCL/fibrinogen blended fibrous scaffolds evaluated by live/dead assays and confocal microscopy. (a) Pure PLCL. (b) PLCL/fibrinogen, 4:1. (c) PLCL/fibrinogen, 2:1. (d) PLCL/fibrinogen, 1:1. (e) PLCL/fibrinogen, 1:2. (f) Pure fibrinogen. Scale bars, 100 μm .

ious biological surfaces [18,30,31]. In our studies, the cell culture experiments also indicated that the fibrinogen in the blended scaffolds enabled us to promote cell proliferation, and the one with PLCL/fibrinogen (2:1) might offer the most suitable qualification for cell culture.

Furthermore, our results for cell viability were roughly in accordance with our results for cell proliferation, which we obtained through WST-8 assays. As shown in Fig. 3, nearly all the cells remained viable (green staining), and very few dead cells (red staining) were detected. This suggests that the electrospun nanofi-

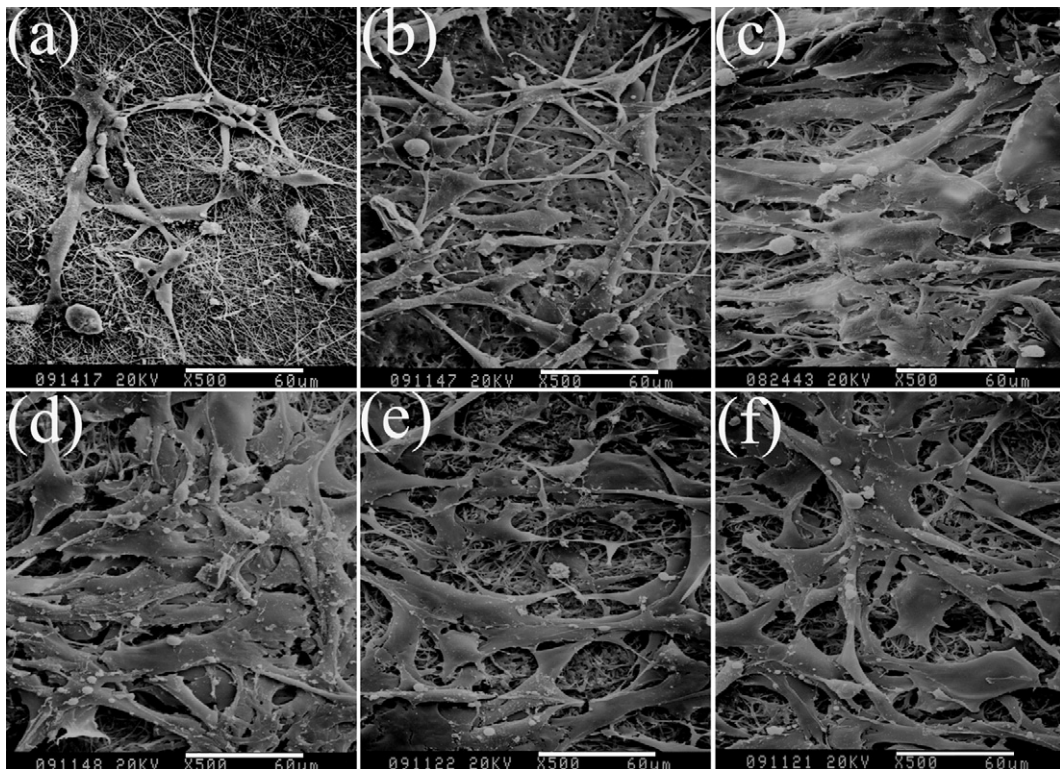


Fig. 4. SEM micrographs of HUVECs cultured on electrospun PLCL/fibrinogen blended fibrous scaffolds. (a) Pure PLCL. (b) PLCL/fibrinogen, 4:1. (c) PLCL/fibrinogen, 2:1. (d) PLCL/fibrinogen, 1:1. (e) PLCL/fibrinogen, 1:2. (f) Pure fibrinogen. Scale bars, 60 μm .

brous scaffolds and their degradation products were relatively non-cytotoxic and suitable for cell culture. Moreover, the densities of the viable cells on the blended nanofibrous scaffolds, especially those on PLCL/fibrinogen (2:1) and PLCL/fibrinogen (1:1) scaffolds (Fig. 3c, d), were higher than those on the pure PLCL scaffolds (Fig. 3a).

In order to analyze the morphological change of cells on nanofibrous, the morphologies of the HUVECs after seven days were observed through SEM. As shown in Fig. 4, fewer HUVECs attached to the pure PLCL nanofibers, and they retained their normal spindle shapes (Fig. 4a) compared with the blended nanofibers and pure fibrinogen nanofibers, on which the cells were much denser and widely spread (Fig. 4b–f). In particular, the HUVECs were well-spread with polygonal shapes, formed multiple cell layers, and reached subconfluence on the PLCL/fibrinogen (2:1) and PLCL/fibrinogen (1:1) scaffolds (Fig. 4c and d). These SEM micrographic observations support the trend of HUVECs proliferation quantified by the WST-8 assays.

4. Conclusions

In the present study, we fabricated novel composite nanofibrous scaffolds by electrospinning blended solutions of PLCL and fibrinogen. We showed that the properties of the resulting nanofibrous scaffolds were strongly influenced by the concentration of fibrinogen in the composite. It was found that the electrospun PLCL/fibrinogen scaffolds provided good support for cell growth, favorable interaction between cell-cell and cell-matrix. Our experimental data demonstrate that the electrospun PLCL/fibrinogen blended nanofibrous scaffolds have great potential for tissue engineering applications in the future.

Acknowledgments

The authors gratefully acknowledge funding from the National High Technology Research and Development Program of China (2007AA03Z429).

References

- [1] Z. Ma, M. Kotaki, R. Inai, S. Ramakrishna, *Tissue Eng.* 11 (2005) 101–109.
- [2] F.C. Pavia, V. La Carrubba, S. Piccarolo, V. Brucato, *J. Biomed. Mater. Res. A* 86 (2008) 459–466.
- [3] G.M. Hoben, J.C. Hu, R.A. James, K.A. Athanasiou, *Tissue Eng.* 13 (2007) 939–946.
- [4] T.J. Sill, H.A. von Recum, *Biomaterials* 29 (2008) 1989–2006.
- [5] S. Sell, C. Barnes, M. Smith, M. McClure, P. Madurantakam, J. Grant, M. McManus, G. Bowlin, *Polym. Int.* 56 (2007) 1349–1360.
- [6] I.K. Kwon, S. Kidoaki, T. Matsuda, *Biomaterials* 26 (2005) 3929–3939.
- [7] E.D. Boland, T.A. Telemeco, D.G. Simpson, G.E. Wnek, G.L. Bowlin, *J. Biomed. Mater. Res. B Appl. Biomater.* 71 (2004) 144–152.
- [8] X.M. Mo, C.Y. Xu, M. Kotaki, S. Ramakrishna, *Biomaterials* 25 (2004) 1883–1890.
- [9] L. Buttafoco, N.G. Kolkman, A.A. Poot, P.J. Dijkstra, I. Vermes, J. Feijen, *J. Controlled Release* 101 (2005) 322–324.
- [10] K. Desai, K. Kit, J. Li, S. Zivanovic, *Biomacromolecules* 9 (2008) 1000–1006.
- [11] S.I. Jeong, S.H. Kim, Y.H. Kim, Y. Jung, J.H. Kwon, B.S. Kim, Y.M. Lee, *J. Biomater. Sci. Polym. Ed.* 15 (2004) 645–660.
- [12] J. Xie, Y. Jung, S.H. Kim, Y.H. Kim, T. Matsuda, *Tissue Eng.* 12 (2006) 1811–1820.
- [13] H.S. Koh, T. Yong, C.K. Chan, S. Ramakrishna, *Biomaterials* 29 (2008) 3574–3582.
- [14] T.G. Kim, T.G. Park, *Tissue Eng.* 12 (2006) 221–233.
- [15] Q. Shi, X. Chen, T. Lu, X. Jing, *Biomaterials* 29 (2008) 1118–1126.
- [16] Y. Zhang, H. Ouyang, C.T. Lim, S. Ramakrishna, Z.M. Huang, *J. Biomed. Mater. Res. B Appl. Biomater.* 72 (2005) 156–165.
- [17] A.H. Henschen, *Thromb. Haemost.* 70 (1993) 42–47.
- [18] M.C. McManus, E.D. Boland, D.G. Simpson, C.P. Barnes, G.L. Bowlin, *J. Biomed. Mater. Res. A* 81 (2007) 299–309.
- [19] S.A. Sell, M.P. Francis, K. Garg, M.J. McClure, D.G. Simpson, G.L. Bowlin, *Biomed. Mater.* 3 (2008) 45001.
- [20] G.E. Wnek, M.E. Carr, D.G. Simpson, G.L. Bowlin, *Nano Lett.* 3 (2003) 213–216.
- [21] C.K. Griffith, C. Miller, R.C. Sainson, J.W. Calvert, N.L. Jeon, C.C. Hughes, S.C. George, *Tissue Eng.* 11 (2005) 257–266.
- [22] L.S. Nair, S. Bhattacharyya, J.D. Bender, Y.E. Greish, P.W. Brown, H.R. Allcock, C.T. Laurencin, *Biomacromolecules* 5 (2004) 2212–2220.
- [23] J.M. Deitzel, J. Kleinmeyer, D. Harris, N.C.B. Tan, *Polymer* 42 (2001) 261–272.
- [24] S. Wongsasulak, K.M. Kit, D.J. McClements, T. Yoovidhya, J. Weiss, *Polymer* 48 (2007) 448–457.
- [25] R. Chen, L. Qiu, Q. Ke, C. He, X. Mo, *J. Biomater. Sci. Polym. Ed.* 20 (2009) 1513–1536.
- [26] H. Zhao, L. Ma, Y. Gong, C. Gao, J. Shen, *J. Mater. Sci. Mater. Med.* 20 (2009) 135–143.
- [27] L. Wu, H. Li, S. Li, X. Li, X. Yuan, Y. Zhang, *J. Biomed. Mater. Res., A* 92 (2010) 563–574.
- [28] S. Zhou, H. Peng, X. Yu, X. Zheng, W. Cui, Z. Zhang, X. Li, J. Wang, J. Weng, W. Jia, F. Li, *J. Phys. Chem. B* 112 (2008) 11209–11216.
- [29] C.H. Kim, M.S. Khil, H.Y. Kim, H.U. Lee, K.Y. Jahng, *J. Biomed. Mater. Res. B Appl. Biomater.* 78 (2006) 283–290.
- [30] Q. Ye, G. Zund, P. Benedikt, S. Jockenhoevel, S.P. Hoerstrup, S. Sakyama, J.A. Hubbell, M. Turina, *Eur. J. Cardiothorac. Surg.* 17 (2000) 587–591.
- [31] D.D. Swartz, J.A. Russell, S.T. Andreadis, *Am. J. Physiol. Heart Circ. Physiol.* 288 (2005) H1451–1460.